FLATNESS BASED CONTROL OF A BUCK-CONVERTER DRIVEN DC MOTOR

Felix Antritter [*,1] **Peter Maurer** [*] **Johann Reger** [**,2]

[*] *Lehrstuhl für Regelungstechnik, Universität Erlangen-Nürnberg, Cauerstrasse 7, D-91058 Erlangen*
[**] *Automatisierungs- und Regelungstechnik, Universität der Bundeswehr München, Werner-Heisenberg-Weg 39, D-85579 Neubiberg*

Abstract: The aim of this contribution is to give a detailed account on the circuit and control design of a buck converter driven DC motor. The steps of design, as for example the choice of the coil, the switching devices employed are discussed at length, all in view of the control objective: tracking control of the DC motor's shaft angular velocity. The dynamic system composed from converter/motor is shown to be differentially flat viewed from the angular velocity, which is a flat output. It is thus possible to derive a flatness-based tracking controller which achieves favorable properties like a smooth starting trajectory for the angular velocity.

Keywords: buck converter, DC motor, tracking control, differential flatness, power electronics, PWM switching, averaged model

1. INTRODUCTION

DC motors are most commonly driven by PWM-signals with respect to the motor input voltage. However, the underlying hard switching strategy causes unsatisfactory dynamic behaviour. The resulting trajectories exhibit a very noisy shape. This causes large forces acting on the motor mechanics and also large currents which detrimentally stress the electronic components of the motor as well as of the power supply. Since it is usually necessary to add a power supply component, anyway, this contribution shall present a control for the entire system, buck-converter/DC Motor. The combination of DC to DC power converters with DC motors has been reported in (Boldea and Nasar, 1999). In particular, the composition of a buck converter with a DC motor has been proposed in (Linares-Flores and Sira-Ramirez, 2004*b*; Linares-Flores and Sira-Ramirez, 2004*a*). The buck type switched DC to DC converter is well known in power-electronics. Due to the fact that the converter contains two energy storing elements, a coil and a capacitor, smooth DC output voltages and currents with very small current ripple can be generated. In this respect, an important issue is the circuit design of the converter in order to obtain, at any time, a high power conversion rate when tracking smooth reference trajectories of the angular velocity. Therefore, this stage is discussed in detail. The outline of the paper is as follows: In Section 3 the circuit design of the buck type power converter is presented, particularly for driving dc motors. In Section 4 an appropriate overall system model is derived for the control design based on the notion of differential flatness (Section 5). It is shown that the overall system model, i.e. of the buck converter with motor, is

[1] email: felix.antritter@rt.eei.uni-erlangen.de, Tel.:+49 (0)9131 8527144
[2] email: johann.reger@unibw.de, Tel.:+49 (0)89 6004 3986

differentially flat with the angular velocity of the motor shaft as a flat output. This allows to pursue the standard flatness-based tracking control strategy for assigning smooth reference trajectories for the angular velocity. A rest to rest transition of the shaft velocity demonstrates the ease of use within the afore-presented control. The measurements presented in Section 6 verify that the overall system yields considerable benefits with respect to smoothness of the angular velocity obtained as well as with respect to the control performance.

2. DC MOTOR

In the practical setup, a DC motor (of type Dunkermotoren) for 24 V/14 W (nominal values) is used. This motor carries a maximum armature current of 4 A. From the respective motor data the converter parameters will be derived in the next section. The motor is equipped with an additional tacho generator to measure the angular velocity of the shaft which is needed for the controller implementation (see Section 6).

3. DESIGN OF THE BUCK-CONVERTER

3.1 Basic Structure

The buck converter (see Figure 1) transforms a certain input voltage U_e into a lower output voltage U_a. To this end, the MOSFET S is driven

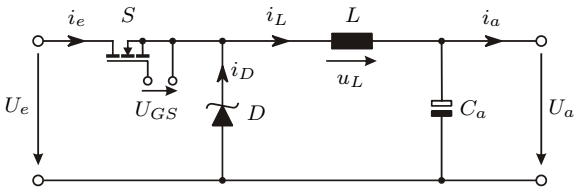

Fig. 1. Buck converter topology

with a PWM-signal. It can be shown that in steady-state the output voltage depends linearly on the duty ratio δ, that is

$$U_a = \delta U_e, \quad 0 \leq \delta \leq 1 \tag{1}$$

The buck converter has two operation modes. In the first mode the MOSFET S is switched on. In this operation mode, the current in the coil increases. When the MOSFET is switched off the current decreases again. Figure 2 shows typical voltage and current diagrams of a buck converter when used in the so-called continuous operation mode, i.e. when $i_L > 0\,\text{A}$ holds over a full period. Due to this switching of the operation mode the coil current exhibits a current ripple Δi_L. But in contrast to the case when direct PWM-switching of the motor voltage is used to generate a desired average motor current, the current ripple in the buck converter can be assigned to an almost arbitrary small value by a proper choice of the coil parameters. For a well dimensioned capacitor C_a the output voltage can be assumed to be constant, with its value corresponding to (1). For the converter, a switching frequency of $f = 45\,\text{kHz}$ has been used. As input voltage $U_e = 24\,\text{V}$ has been used since this is the maximum voltage of the DC motor (see Section 2)

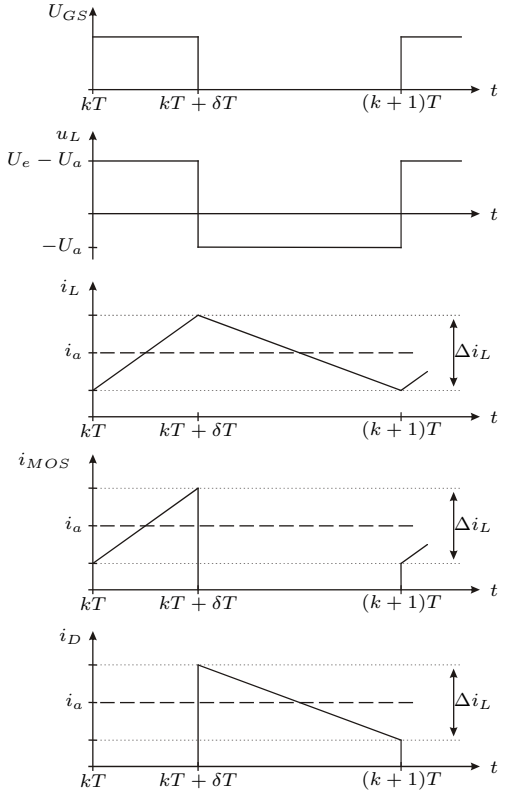

Fig. 2. Voltages and currents in continuous mode

3.2 Design of the Coil

As mentioned above, the current ripple Δi_L of the buck converter depends on the inductance of the coil. The relation is given by

$$\Delta i_L = \frac{1}{L} \cdot (U_e - U_a) \cdot \frac{\delta}{f} \tag{2}$$

(see (Kories and Schmidt-Walter, 2004)). Solving this equation for L expresses the inductance of the coil in terms of the admissible current ripple Δi_L. In order to ensure that the converter is always in continuous mode the minimal average output current is taken to be the motor current when running idle. This current is about 0.1 A. Thus, a choice of $\Delta i_L = 0.2\,\text{A}$ would be admissible. For achieving even smoother currents Δi_L is set to 0.1 A. The necessary inductance according to (2) also depends on U_a which is varying. So, to assure $\Delta i_L \leq 0.1\,\text{A}$ for all possible output voltages, $U_a = U_e/2$ is chosen which maximizes the right hand side of (2). Thus, the necessary inductance results in

$$L = \frac{U_e}{4 \cdot f} \cdot \frac{1}{\Delta i_L} = 1.33\,\text{mH} \tag{3}$$

where moreover $\delta = U_a/U_e$ from (1) was inserted. Practically, the coil has been realized using a ferrite core with an air gap of 1 mm which, for the used number of windings, avoids saturation effects of the core for current levels up to 4 A. The ohmic resistance of the coil is about $R_L = 0.2\,\Omega$. A larger inductance as specified in (3) should not be used because this may only be realized with an increased number of coil windings which would lead to increasing ohmic losses; all the more as higher inductances have to be realized with bigger air gaps in the core to prevent saturation effects. This again would lead to even more windings.

3.3 Output Filter

The coil and the capacitor at the converter output form a low pass that may filter high-frequency disturbances caused by the PWM-switching of the MOSFET S. The cut-off frequency of the filter is given by

$$f_{co} = \frac{1}{2\pi\sqrt{LC_a}} \tag{4}$$

As a rule of thumb, the cut-off frequency is taken to be about a factor $10^{-2} \ldots 10^{-3}$ smaller than the switching frequency. With (4) and the beforehand calculated inductance this leads to

$$94\mu F \;\leq\; C_a \;\leq\; 9400\mu F \quad . \tag{5}$$

For preserving an acceptable dynamic behaviour in the setup the capacitance is chosen in the lower region, here $C_a = 470\,\mu$F.

3.4 Switching Devices

The main issues for the choice of the switching device are the reduction of switching losses and the dimensioning for the necessary currents. Thus, a MOSFET with low $R_{DS(on)}$ is chosen. The used MOSFET shows an $R_{DS(on)} = 77\,\mathrm{m}\Omega$ and can thus handle easily the maximum current of 4 A. Furthermore, due to the fact that to be switched on the MOSFET needs a positive voltage $U_{GS} > 0$ it follows that the potential of the MOSFET gate to ground has to be even higher than U_e when switching on the MOSFET. Therefore, a so called "level-shifter" has to be used. This device allows its output voltage, used to switch the MOSFET, to be higher than its input supply voltage. The level shifter also achieves very short rise and fall times for the switching of the MOSFET. This reduces the switching losses in the device.

The diode has to handle a reverse voltage that is equal to the input voltage U_e of the converter. For keeping losses low a schottky barrier diode is employed since it is associated to a low forward voltage and a small reverse recovery time.

3.5 Sensors

In the setup, the capacitor voltage u_C, the coil current i_L and the output current i_A are measured with measurement amplifiers. In order to measure current via voltage the addtional resistances R_4 and R_6 are introduced for the measurement of i_L and i_A, see Figure 4. For reducing losses, the ohmic resistances are set to only $R_4 = R_6 = 10\,\mathrm{m}\Omega$.

3.6 Measurements

The measurements depicted in Figure 3 show that the converter output voltage indeed linearly depends on the duty ratio δ. For demonstration that only very small losses occur in the converter an output current of $3\,A$ was adjusted using an ohmic resitance as load at a duty ratio of $\delta = 1$. Due to the low ohmic resistances of the MOSFET and of the coil the output voltage $U_a = 23.04\,V$ is only slightly smaller than the input voltage $U_e = 24\,V$. At this operating point the power conversion ratio has been determined to be

$$\eta = \frac{P_{out}}{P_{in}} = 0.96 \tag{6}$$

The measurement shows that even at high power

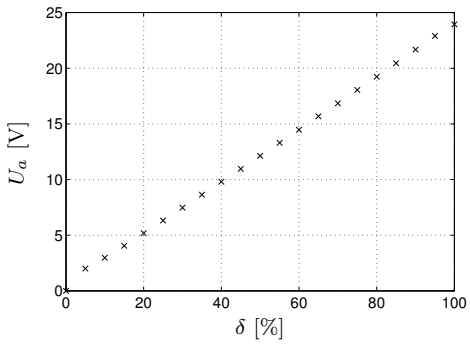

Fig. 3. steady state converter output voltage U_a as a function of the duty ratio when connecting an ohmic resistor of $140\,\Omega$ as load

levels the converter is able to transfer almost the complete input voltage U_e to the output. Thus, with this converter design no performance limitations should be imposed on the motor.

4. DYNAMIC MODEL OF THE BUCK CONVERTER WITH MOTOR

A simplified model of the overall system buck-converter/DC-motor is shown in Figure 4. The switching devices have been replaced by an ideally switched voltage source. This is indicated by the multiplication of U_e with the switching variable $u \in \{0, 1\}$. An additional resistance R_L has been added to the model in order to take into account the ohmic resistence of the coil windings. The

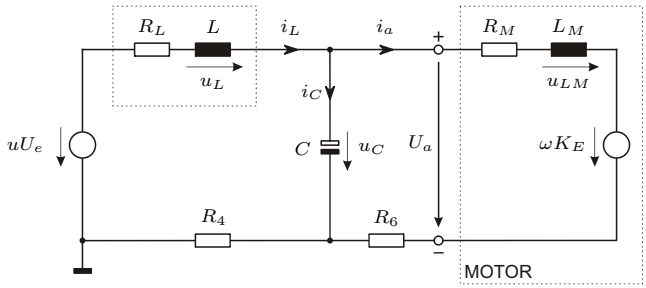

Fig. 4. Overall layout of the buck converter with motor

motor has been modeled by an inductance L_M with ohmic resistance R_M and electromagnetic voltage source ωK_E, where the parameters have been determined as $L_M = 8.9\,\mathrm{mH}$, $R_M = 6\,\Omega$, and $K_E = 0.0517\,\frac{\mathrm{V}}{\mathrm{rad/sec}}$. Completing the model with the mechanical equation that describes the dynamics of the motor shaft, a linear 4th order system

$$\dot{x} = Ax + Bu \tag{7}$$

results where

$$x = \begin{pmatrix} i_L & u_C & i_a & \omega \end{pmatrix}^T \tag{8}$$

$$A = \begin{pmatrix} \frac{-R_L}{L} & \frac{-1}{L} & 0 & 0 \\ \frac{1}{C} & 0 & \frac{-1}{C} & 0 \\ 0 & \frac{1}{L_M} & \frac{-R_M}{L_M} & \frac{-K_E}{L_M} \\ 0 & 0 & \frac{K_M}{J} & 0 \end{pmatrix} \tag{9}$$

$$B = \begin{pmatrix} \frac{U_e}{L} & 0 & 0 & 0 \end{pmatrix}^T \tag{10}$$

The moment of inertia of the motor with tacho generator has been determined to be $J = 7.95 \cdot 10^{-6}\,\mathrm{kg \cdot m^2}$ and $K_M = 0.0517\frac{\mathrm{Nm}}{A}$. In (8)–(10) the very low measurement amplifier resistances R_4 and R_6 (see Section 3.5) have been neglected.

Acoording to (Ortega *et al.*, 1998) the discrete input $u \in \{0, 1\}$ can be replaced with the duty ratio $\delta \in [0, 1]$ when using a PWM-strategy to generate δ from an analog input signal. Hence, for the given setup we may refer to a so-called averaged dynamic model, given by

$$\dot{x} = Ax + B\delta \tag{11}$$

where the new input is the duty ratio δ.

Note that this linear system description is valid only as long as it can be ensured that no saturation effects occur in the coil. Otherwise the inductance L would depend nonlinearly on the current i_L.

5. CONTROLLER DESIGN

5.1 Flatness-based Tracking Controller Design

Recalling basic notions from (Fliess *et al.*, 1995), an n-th order single input single output system

$$\dot{x} = f(x, u) \tag{12}$$

is (differentially) flat if there exists a scalar output

$$y_f = \Phi(x) \tag{13}$$

called flat output, which allows a differential parameterization of the states and the inputs as per

$$x = \psi_x(y_f, \dot{y}_f, \ldots, y_f^{(n-1)}) \tag{14}$$

$$u = \psi_u(y_f, \dot{y}_f, \ldots, y_f^{(n)}) \tag{15}$$

Relations (14)–(15) can be used for feedforward and feedback tracking controller design. This is outlined in the following.

5.2 Flatness of the Buck-converter with DC Motor

For linear systems the concept of flatness is equivalent to controllability (Fliess *et al.*, 1995). Referring to (Sira-Ramirez and Agrawal, 2004) a flat output candidate is given by the inner product of the last row of the inverse of the Kalman controllability matrix and the state vector. The controllability matrix of the fourth order system (11) reads

$$Q_C = \begin{bmatrix} B & AB & A^2B & A^3B \end{bmatrix} \tag{16}$$

and is nonsingular, as can be verified easily. Therefore, a possible flat output is

$$y_{f0} = \begin{bmatrix} 0 & 0 & 0 & 1 \end{bmatrix} Q_C^{-1} x = \frac{JL_MCL}{K_M U_e}\omega \tag{17}$$

Instead of y_{f0} any non-trivial scalar multiple can be taken as an other flat output, that is, the angular velocity

$$y_f = \omega = \underbrace{\begin{bmatrix} 0 & 0 & 0 & 1 \end{bmatrix}}_{C_f} x \tag{18}$$

is a flat output. A transformation of system (11) into controller normal form is given by

$$\begin{aligned} z &= \begin{bmatrix} z_1 & z_2 & z_3 & z_4 \end{bmatrix}^T = \begin{bmatrix} y_f & \dot{y}_f & \ddot{y}_f & y_f^{(3)} \end{bmatrix}^T \\ &= \begin{bmatrix} C_f & C_fA & C_f^2A & C_f^3A \end{bmatrix} x = Tx \end{aligned} \tag{19}$$

(see (Sira-Ramirez and Agrawal, 2004)). The transformed system

$$\dot{z} = TAT^{-1}z + TB\delta \tag{20}$$

consequently, is in controller normal form and the differential parameterization of the input is given by solving the last row of (20) for δ, which yields

$$\delta = \psi_\delta(z, \dot{z}_4) \tag{21}$$

Equations (18) and (21) together with the inverse of (19)

$$x = T^{-1}z \tag{22}$$

establish the relations (13)–(15).

5.3 Reference Trajectory

Regulating a DC motor from initial rest, i.e. when the initial angular velocity is zero, to some desired final angular velocity may cause very inconvenient transient behaviour. In order to verify that the proposed approach allows to achieve very smooth

transitions, a smooth start from steady state $\omega = 0$ to a final angular velocity (steady state) shall be planned. The corresponding reference trajectory $y_{f,d}$ for the output is associated to the boundary conditions

$$y_{f,d}(0) = 0, \qquad y_{f,d}(T_f) = \omega_e \tag{23}$$

and

$$y_{f,d}^{(i)}(0) = 0, \quad y_{f,d}^{(i)}(T_f) = 0, \quad i = 1,2,3 \tag{24}$$

In view of (19) the conditions (24) follow from the fact that the system is transferred from one stationary point to another. To realize a trajetory which satisfies the conditions (23)–(24) an 11th order polynomial has been used, which also satisfies

$$y_{f,d}^{(4)}(0) = y_{f,d}^{(4)}(T_f) = y_{f,d}^{(5)}(0) = y_{f,d}^{(5)}(T_f) = 0 \tag{25}$$

The duration T_f of the reference trajectory is chosen such that the bound $\delta_d \in [0,1]$ can be assured.

6. TRACKING PERFORMANCE

6.1 Feedforward Controller

A feedforward tracking controller is obtained by inserting the reference trajectory $y_{f,d}$ into the differential parameterization (21) of the input δ

$$\delta_d = \psi_\delta(z_d, \dot{z}_{4,d}) \tag{26}$$

in view of (19). Having taken into account the boundary conditions (24)–(25) guarantees that the feedforward (26) is sufficiently continuously differentiable. Figure 5 shows the resulting measurements with the laboratory setup when $T_f = 0.2\,\text{sec}$. Due to modelling errors the angular velocity does not track exactly the assigned trajectory. However, the deviations are not very large and the basic shape of the trajectory resembles quite well the shape of the assigned trajectory. Particularly, the trajectory for the angular velocity is smooth and thus the stresses on the mechanics and the electric components of the motor are reduced to a minimum.

6.2 Feedback Tracking Controller

For the stabilization of the reference trajectory, an addtional feedback controller can be realized using flat feedback. When replacing $\dot{z}_4$ by the new input v in (21) the feedback law reads

$$\delta = \psi_\delta(z, v) \tag{27}$$

Substituting (27) into (20) yields the Brunovsky normal form

$$\begin{aligned} \dot{z}_i &= z_{i+1}, \quad i = 1,2,3 \\ \dot{z}_4 &= v \end{aligned} \tag{28}$$

Defining the tracking error

$$e_1 = y_f - y_{f,d} \tag{29}$$

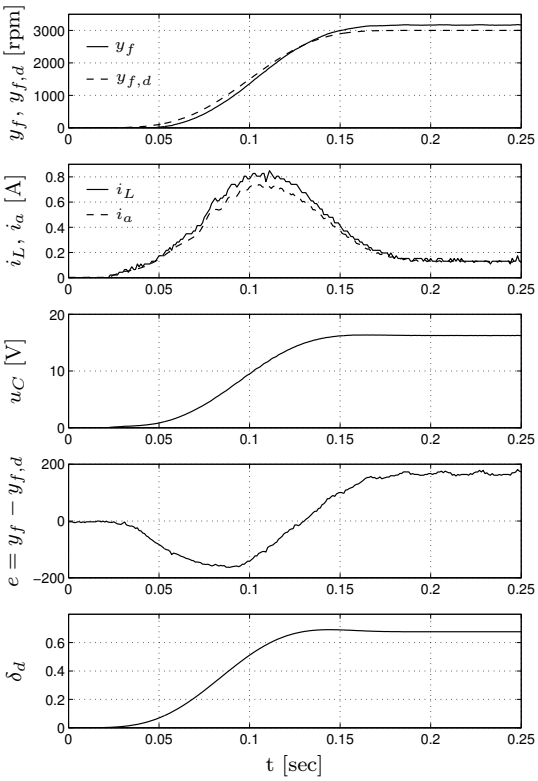

Fig. 5. Smooth start with the feedforward controller for laboratory setup

then with (28) the tracking error system results in

$$\begin{aligned} \dot{e}_i &= e_{i+1}, \quad i = 1,2,3 \\ \dot{e}_4 &= v - y_{f,d}^{(4)} \end{aligned} \tag{30}$$

Thus, by assigning to v the feedback

$$v = y_{f,d}^{(4)} - \Lambda(e) \tag{31}$$

with

$$\Lambda(e) = \lambda_4 e_4 + \lambda_3 e_3 + \lambda_2 e_2 + \lambda_1 e_1 + \lambda_0 \int_0^t e_1(\tau)d\tau \tag{32}$$

and in view of (30) the tracking error dynamics

$$e_1^{(4)} + \lambda_4 \dddot{e}_1 + \lambda_3 \ddot{e}_1 + \lambda_2 \dot{e}_1 + \lambda_1 e_1 + \lambda_0 \int_0^t e_1(\tau)d\tau = 0 \tag{33}$$

are obtained. Due to the feedback of the integral tracking error of the angular velocity, this controller achieves asymptotic tracking even in the presence of model errors or load torque disturbances. Figure 6 shows mesurements which result from applying the feedback tracking controller (27), (31) with all the roots of the characteristic polynomial of (33) beeing placed at -450 to the laboratory setup. In Figure 7 a load torque is applied to the controlled system. In this case the controller (27), (31) is used to stabilize a constant angular velocity of 3000 rpm. It can be seen that the feedback controller very well rejects the disturbance and only a very small and short-time deviation from the desired angular velocity

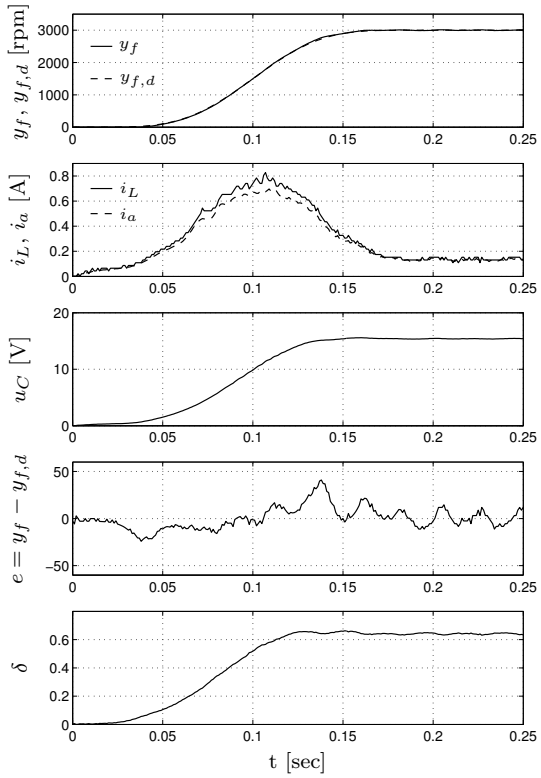

Fig. 6. Smooth start with the feedback controller for laboratory setup

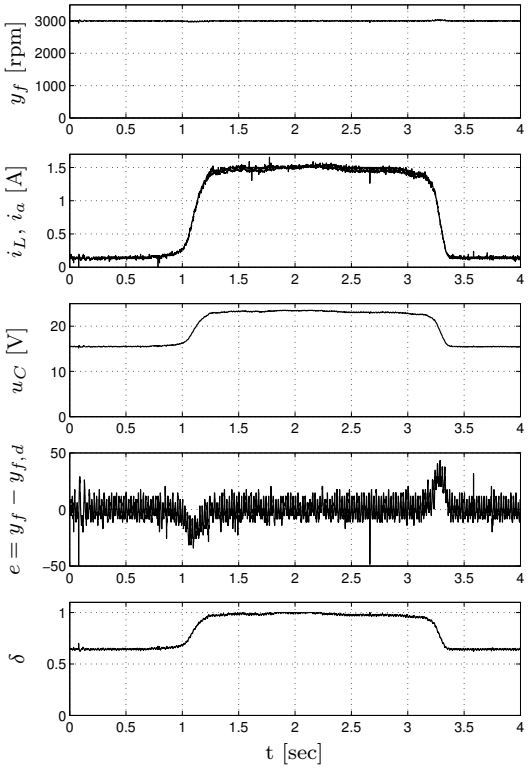

Fig. 7. Measured trajectories for a constant angular velocity reference stepwize load torque change (feedback controller)

of 3000 rpm occurs. Looking at the duty ratio it can be verified that the motor is at the limit of its capability when the load torque is applied. This impressively shows the advantages of the flatness-based control policy on a buck converter steered DC motor setup.

7. CONCLUSIONS

A flatness-based tracking controller for a buck converter driven DC motor has been derived. The crucial steps within the circuit design of the buck converter have been illustrated in detail. The overall system model has been shown to be differentially flat with flat output the angular shaft velocity, which is supposed to be measured. Thus, it was possible to design a flatness-based tracking controller for the angular velocity. It could be shown that already the pure feedforward controller resulted in very satisfactory trajectories for the angular velocity. The excellent tracking behaviour and disturbance rejection of the feedback tracking controller has also been demonstrated by means of measurements on a laboratory setup. One future task is to improve the controller by using (dynamic) output feedback, only. This may be carried out in various ways, but in any case will help reduce the number of states to be measured. Another task is to extend the setting to a broader class of power-converter/drive combinations. In general, this combination may lack the flatness property which entails the need for other control policies, as for example passivity (Linares-Flores *et al.*, 2006).

REFERENCES

Boldea, I. and S.A. Nasar (1999). *Electric Drives*. CRC Press LLC. Boca Raton.

Fliess, M., J. Lévine, P. Martin and P. Rouchon (1995). Flatness and defect of nonlinear systems: introductory theory and examples. *Int. J. Control* **61**, 1327–1361.

Kories, R. and H. Schmidt-Walter (2004). *Taschenbuch der Elektrotechnik*. Harri Deutsch Verlag. Berlin.

Linares-Flores, J. and H. Sira-Ramirez (2004*a*). Dc motor velocity control through a dc-to-dc power converter. *Proceedings of 43rd Conference on Decision and Control (CDC)* **5**, 5297–5302.

Linares-Flores, J. and H. Sira-Ramirez (2004*b*). A smooth starter for a dc machine: a flatness based approach. *Proceedings of 1st International Conference on Electrical and Electronics Engineering and X Conference on Electrical Engineering* pp. 589–594.

Linares-Flores, J., J. Reger and H. Sira-Ramirez (2006). A time-varying linear state feedback tracking controller for a boost-converter driven dc machine. *Proceedings of 4th IFAC-Symposium on Mechatronic Systems*.

Ortega, R., A. Loria, P.J. Nicklasson and H. Sira-Ramirez (1998). *Passivity-based Control of Euler-Lagrange Systems*. Springer. London.

Sira-Ramirez, H. and S. K. Agrawal (2004). *Differentially Flat Systems*. Marcel Dekker. New York.